Determination of 70-Meter Antenna Elevation-Axis Inertia

J. Sommerville[1]

In the near future, JPL will create spacecraft/transmitters that are smaller in size to reduce mission costs significantly. However, a smaller spacecraft transmitter/dish creates a signal that is smaller in wavelength. The Earth-based 70-m downlink antenna cannot track smaller wavelengths, unless improvements are made to the current servo system. A study is conducted to define some 70-m antenna servo system parameters that will allow improvements in its tracking response for smaller targets.

I. Introduction

Plans are under way to upgrade the 70-m antenna from the current 8 MHz (X-band) to 32 MHz (Ka-band). The Ka-band wavelength is one-fourth the size of the current X-band wavelength. This means that the 70-m antenna must point to a smaller target. The 70-m antenna pointing accuracy and tracking response must be improved to operate within the Ka-bandwidth. The 70-m antenna's tracking response can be improved by minimizing the time it takes to respond to external disturbances such as wind. Excessive inertia on the servo drive motors causes the antenna to sluggishly correct its pointing position when wind disturbances move the antenna position away from its intended path. In this article, the 70-m elevation-axis inertia is determined to provide a baseline for the existing servo control system. The baseline data will be used as reference to make servo system design improvements. Industrial servo control experts recommend that the servo motor's inertia should equal or match the inertia of the reflected load. The term "inertia matching" is the practice of balancing the inertia of a servo motor with the load inertia (i.e., the inertia that is felt by the servo motor). A parallel effort is under way to define the best inertia ratio for the 70-m antenna requirements. The primary purpose of this article is to quantify the existing 70-m elevation-axis inertia. A secondary purpose is to compare the current 70-m inertia ratios to the proposed 70-m inertia ratios and to the former 64-m inertia ratio values.

Three approaches were taken to determine the current 70-m antenna's effective inertia for the elevation axis. The first method determines inertia by analysis of the antenna's mass properties and gear ratios. The mass properties are estimated from component geometry that is depicted in drawings and from mass properties data supplied by JPL's Antenna Mechanical Structural Engineering Group.

---

[1] Communications Ground Systems Section.

The research described in this publication was carried out by the Jet Propulsion Laboratory, California Institute of Technology, under a contract with the National Aeronautics and Space Administration.

The second method derives a mathematical expression for the hydraulic natural frequency. Then, the antenna reflected inertia, J, is calculated from the same expression. Test data are used to determine the hydraulic stiffness, K, and the hydraulic natural frequency, f:

$$f_{\text{hydraulic}} = \frac{1}{2\pi}\sqrt{\frac{K}{J}} \tag{1}$$

The system rotational inertia is then calculated from the rearranged formula for the hydraulic natural frequency:

$$J = \frac{K}{\left(2\pi f_{\text{hydraulic}}\right)^2} \tag{2}$$

This method of determination is independent of the antenna's frictions. However, an analysis of the hydraulic motor pressures is necessary. When the antenna is driven, both structural and hydraulic forces are manifested in the hydraulic-line pressure traces. These forces are periodic in nature. The resultant waveform must be decomposed into its component frequencies by using a fast Fourier transform (FFT). Then, the hydraulic resonance frequency must be selected from a number of other resident frequencies in the FFT power spectral density.

The third method used to determine the antenna's inertia is the application of an integrated form of Newton's equation to 70-m antenna-drive test data: $\sum T = J\alpha$ (the summation of torques is equal to rotational inertia times angular acceleration). The integral form of Newton's equation states that the impulse (the integral of applied torques over time) is equal to the change in angular momentum (the antenna inertia times the angular speed) of the antenna. This approach requires some knowledge of all of the antenna external forces, such as the driving forces, offset torques, coulomb and static frictions, etc.

II. Antenna Inertia Calculations from Mass Properties

The antenna inertia is a composite that includes the hydraulic motors, the gearbox pinions and shafts, and the antenna itself. The inertia of each component follows.

The servo motor's inertia encompasses the motor's inertia and any object that is rigidly attached to the motor's shaft. The motor inertia, J_{motor}, is comprised of two components: the motor inertia and the flywheel inertia. The 70-m antenna motors have 24 flywheel disks rigidly coupled to the motor shaft. The load inertia encompasses the gear heads, pinions, and the inertia of the driven load. The amount of inertia felt by the servo motor is called the reflected inertia or effective inertia.

The six elevation-axis rotating assemblies are

$J_1 =$ the inertia of the first intermediate shaft/pinion and the high-speed gear

$J_2 =$ the inertia of the second intermediate shaft/pinion and the first intermediate gear

$J_3 =$ the inertia of the third intermediate shaft/pinion and the second intermediate gear

$J_4 =$ the inertia of the low-speed gear and bull pinion

$J_{ct} =$ the inertia of the counter-torque motor and the high-speed shaft/pinion

$J_{ant} =$ the inertia of the antenna tipping mass

The inertia of each component is reflected to the motor axis by taking into account the gear train ratios; D'Azzo and Houpis [1] developed a mathematical relationship between the gear ratios and the gearbox pinion and shaft inertias:

$$J_{\text{reflected}} = J_{\text{motor}} + J_{ct} + \frac{J_1}{(N_1)^2} + \frac{J_2}{(N_1 N_2)^2} + \frac{J_3}{(N_1 N_2 N_3)^2} + \cdots + \frac{J_{ant}}{(N_1 N_2 N_3 N_4 N_5)^2} \tag{3}$$

The reflected inertia is mathematically represented in Eq. (3). The reflected inertia is the rotating inertia (e.g., motor, gear head, or antenna dish inertias) divided by the square of the ratio of the motor speed to the speed of the gear head or tipping mass. The load inertia, J_L, consists of the six rotating assemblies that are scaled relative to their axis speed ratios. Each of the rotating assemblies has a different rotating speed relative to the motor rate, with the exception of J_{ct}, the counter-torque motor and shaft/pinion. Mathematically, J_L, is defined as the sum of all of the terms on the right-hand side of Eq. (3), less the the first term, J_{motor}.

The inertia values for Eq. (3) are

$J_{ant64m} =$ inertia for 64-m elevation antenna tipping mass, 100×10^6 lbf-ft-s^2 (see Footnote 2)

$J_{ant70m} =$ inertia for 70-m elevation antenna tipping mass, 2.41667×10^8 lbf-ft-s^2

The inertia value for the 64-m azimuth axis is not known. The inertia value for the 70-m azimuth when the elevation axis is positioned at 60 deg is 3.033×10^8 lbf-ft-s^2.

For the elevation axis, the ratios of speeds between the adjoining rotating assemblies are

$N_1 = 134/20$

$N_2 = 101/21$

$N_3 = 113/23$

$N_4 = 77/20$

$N_5 = 754/16$

The inertia of the shaft and gear components may be approximated by that of a solid-steel disk,

$$J_i = \frac{1}{2} M R_i^2 \tag{4}$$

where M is the mass of the disk or shaft and R_i is the outer radius of the disk or shaft. Equation (4) is an overestimation of the pinion gear inertia because each pinion actually has gear teeth cut into its outer edge. A circular disk is chosen as a geometrical approximation to simplify the inertia calculation.

The weight of the disk, W, is calculated by multiplying the specific weight of the disk, ρ, times the volume of the disk, V:

[2] "The NASA/JPL 64-Meter-Diameter Antenna at Goldstone, California: Project Report," Technical Memorandum 33-671 (internal document), Jet Propulsion Laboratory, Pasadena, California, p. 180, July 15, 1974.

$$W = \rho V \tag{5}$$

where ρ for steel is 7832 kg/m^3 (15.28 slug/ft^3) (see [2]),

$$V = \pi R^2 H \tag{6}$$

R is the radius of the disk, and H is the thickness or length of the disk.

Table 1 lists the assumed dimensions of the shafts and gears of the rotating assemblies.

Table 1. Rotating assembly inertias.

Rotating assembly	Radius, cm (in.)	Length/ thickness, cm (in.)	Inertia component, $1/2\,MR^2, J_{ii}$, kg-m^2 (lbf-ft-s^2)	Composite inertia, J_i, kg-m^2 (lbf-ft-s^2)
(1) Inertia of the first intermediate shaft/ pinion and the high-speed gear	Shaft/pinion: 3.81 (1.5)	38.1 (15)	$J_{11} = 0.0099$ (0.0073)	$J_1 = J_{11} + J_{12}$ 1.5876 (1.1710)
	Gear: 22.42 (8.827)	5.08 (2)	$J_{12} = 1.5777$ (1.1637)	
(2) Inertia of the second intermediate shaft/ pinion and the first intermediate gear	Shaft/pinion: 6.667 (2.625)	34.29 (13.5)	$J_{21} = 0.075518$ (0.0557)	$J_2 = J_{21} + J_{22}$ 5.2576 (3.8779)
	Gear: 26.67 (10.5)	8.255 (3.25)	$J_{22} = 5.182$ (3.8221)	
(3) Inertia of the third intermediate shaft/ pinion and the second intermediate gear	Shaft/pinion: 10.795 (4.25)	49.53 (19.5)	$J_{31} = 0.7688$ (0.5671)	$J_3 = J_{31} + J_{32}$ 31.294 (23.0816)
	Gear: 36.4998 (14.375)	13.97 (5.5)	$J_{32} = 30.525$ (22.5144)	
(4) Inertia of the low-speed gear and bull pinion	Shaft/pinion: 26.162 (10.3)	68.58 (27)	$J_{41} = 39.49798$ (29.1326)	$J_4 = J_{41} + J_{42}$ 194.5418 (143.4886)
	Gear: 49.53 (19.5)	20.955 (8.25)	$J_{42} = 155.0439$ (114.356)	
(5) Inertia of the counter-torque motor and the high-speed shaft/ pinion	Shaft/pinion: 3.81 (1.5)	38.61 (15.2)	$J_{C1} = 0.009897$ (0.0073)	$J_C = J_{C1} + J_{C2}$ 0.01207 (0.0089)
	Counter-torque motor	—	$J_{C2} = 0.00021$ (0.00155)	

The load inertia, J_L, is the inertia felt at the motor and is given in Tables 2 and 3 for the 64-m and 70-m antennas, respectively.

Using Eq. (3), one adds the 64-m load inertias from Table 2 to the single motor inertia,

$$J_{\text{motor64m}} = 0.17712 \text{ kg-m}^2 (0.13064 \text{ ft-lbf-s}^2)$$

to obtain the reflected inertias:

Table 2. 64-meter antenna load inertia table.

Item no.	Rotating assembly	Load inertia, kg-m^2 (lbf-ft-s^2)	Load inertia formula, J_i
1	First intermediate shaft/ pinion and the high-speed gear	0.14164 (0.10434)	$4J_1/(N_1)^2$
2	Second intermediate shaft/ pinion and the first intermediate gear	0.0194 (0.01494)	$4J_2/(N_1N_2)^2$
3	Third intermediate shaft/ pinion and the second intermediate gear	0.04989 (0.00368)	$4J_3/(N_1N_2N_3)^2$
4	Low-speed gear and bull pinion	0.002088 (0.00154)	$4J_4/(N_1N_2N_3N_4)^2$
5	Counter-torque motor and the high-speed shaft/pinion	0.048402 (0.03570)	$4J_{ct}$
6	Inertia of the 64-m antenna tipping mass	0.164323 (0.12120)	$J_{ant}/(N_1N_2N_3N_4N_5)^2$
7	Summation of 64-m load inertias	0.3815 (0.28141)	$J_L = \sum_{i=1}^{6} J_i$

$$\text{64-m reflected inertia} = 4 \times 0.17712 + 0.3815 = 1.09 \text{ kg-m}^2$$
$$= 4 \times 0.13064 + 0.28141 = 0.804 \text{ ft-lbf-s}^2$$

The motor-to-load inertia ratio is the motor inertia divided by the load inertia from Table 2:

$$4 \times \frac{J_{\text{motor64m}}}{J_L} = 1.8568$$

for the 64-m antenna (elevation axis).

For the 70-m antenna, one also uses Eq. (3) and adds the load inertias from Table 3 to the single motor inertia,

$$J_{\text{motor70m}} = 0.3007 \text{ kg-m}^2 (0.22177 \text{ ft-lbf-s}^2)$$

to obtain the reflected inertias:

$$\text{70-m antenna reflected inertia} = 4 \times 0.3007 + 0.5732 = 1.7759 \text{ kg-m}^2$$
$$= 4 \times 0.22177 + 0.42282 = 1.31 \text{ ft-lbf-s}^2$$

The motor-to-load inertia ratio is the motor inertia divided by the load inertia from Table 3:

$$4 \times \frac{J_{\text{motor70m}}}{J_L} = 2.09799$$

for the 70-m antenna (elevation axis).

Table 3. 70-meter antenna load inertia table.

Item no.	Rotating assembly	Load inertia, kg-m^2 (lbf-ft-s^2)	Load inertia formula, J_i
1	First intermediate shaft/ pinion and the high-speed gear	0.14146 (0.10434)	$4J_1/(N_1)^2$
2	Second intermediate shaft/ pinion and the first intermediate gear	0.02025 (0.01494)	$4J_2/(N_1N_2)^2$
3	Third intermediate shaft/ pinion and the second intermediate gear	0.004989 (0.00368)	$4J_3/(N_1N_2N_3)^2$
4	Low-speed gear and bull pinion	0.002088 (0.00154)	$4J_4/(N_1N_2N_3N_4)^2$
5	Counter-torque motor and the high-speed shaft/pinion	0.048402 (0.03570)	$4J_{ct}$
6	Inertia of the 70-m antenna tipping mass	0.356047 (0.26261)	$J_{ant}/(N_1N_2N_3N_4N_5)^2$
7	Summation of 70-m load inertias	0.57324 (0.42281)	$J_L = \sum_{i=1}^{6} J_i$

III. Antenna Inertia Calculation from the Hydraulic Natural Frequency

The 70-m antenna rotational inertia will be calculated from the hydraulic resonance equation.

A mathematical relationship for the hydraulic resonance of the 70-m antenna will be developed. The hydraulic natural frequency and hydraulic line stiffness will be determined from spectral analysis of hydraulic line pressure traces. The 70-m antenna has four hydraulic motors that drive four pinions that ultimately turn the large antenna structure on an axis of rotation, as depicted in Fig. 1.

The sum of the hydraulic motor torques equals the reflected motor inertia, J, times the angular acceleration of the motor, $\ddot{\theta}$:

$$\sum T_i = J\ddot{\theta} \tag{7}$$

The torque, T_i, of an individual hydraulic motor is

$$T_i = e_t \frac{d}{2\pi} \Delta p \tag{8}$$

where d is the hydraulic motor volumetric displacement in units of volume per shaft revolution. The variable e_t is the motor's torque efficiency.

Since there are four motors for the four pinions of Fig. 1, the sum of the motor torques becomes

$$\sum T_i = e_t \frac{4d}{2\pi} \left[dp_1 - dp_2\right] \tag{9}$$

where the variables dp_1 and dp_2 represent a small change in pressure inside the common hydraulic lines leading to the motors.

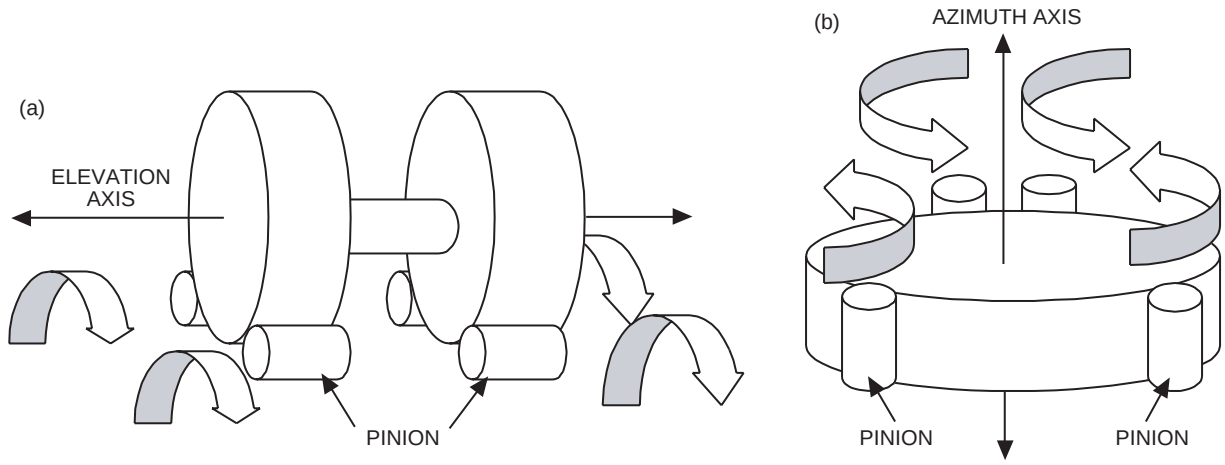

Fig. 1. The 70-m drive pinion and bull gear configuration for the (a) elevation and (b) azimuth axes.

The change in pressure inside the hydraulic line is related to the volume of the line by the bulk modulus, β:

$$\beta = \frac{dp}{\frac{\Delta V}{V}} \tag{10}$$

Solving for the change in line pressure, dp, one obtains

$$dp = \beta \frac{\Delta V}{V} \tag{11}$$

If the hydraulic motor shaft was slightly rotated in a positive direction, a small amount of fluid would be extracted from one hydraulic line, and the same amount of fluid would be added to the other line. Assume that the volume V_2 in the hydraulic schematic loses fluid and the volume V_1 gains fluid. So, the corresponding change in the line pressures would be the following:

$$\left.\begin{aligned} dp_1 &= \beta \frac{\Delta V_1}{V_1} \\ dp_2 &= -\beta \frac{\Delta V_2}{V_2} \end{aligned}\right\} \tag{12}$$

where ΔV_1 is the small amount of fluid added to the volume V_1, and ΔV_2 is the small amount of fluid extracted from volume V_2 when the motor shaft is twisted.

When the hydraulic motor shaft rotates, the amount of fluid that transfers from one side to the other is determined by the motor's displacement, d:

$$d = \frac{\text{fluid}}{\text{shaft}} \tag{13}$$

Let θ represent the angular position of the hydraulic motor. Each hydraulic motor delivers a specified volume of fluid per (2π rad) angular rotation of the motor shaft. In the 70-m hydraulic configuration depicted in Fig. 2, each hydraulic motor moves fluid to or from a common control volume, V_1 or V_2. Thus, Eq. (14) represents the change in volume of ΔV_1 and ΔV_2 as four times the displacement of a single motor times the hydraulic motor's volumetric efficiency, e_v:

$$\left.\begin{aligned} \Delta V_1 &= e_v \frac{4d\theta}{2\pi} \\ \Delta V_2 &= e_v \frac{4d\theta}{2\pi} \end{aligned}\right\} \tag{14}$$

By substituting Eq. (12) for dp_1 and dp_2 into the equation of motion for the antenna, Eq. (9), and then substituting Eq. (14) for volume changes, ΔV_1 and ΔV_2, into the resulting equation, one obtains

$$\sum T_i = e_t e_v \beta \left(\frac{4d}{2\pi}\right)^2 \left[\frac{1}{V_1} + \frac{1}{V_2}\right] \theta = J\ddot{\theta} \tag{15}$$

or,

$$K\theta = J\ddot{\theta} \tag{16}$$

where K is the equivalent hydraulic stiffness of the 70-m antenna:

$$K = e_t e_v \beta \left(\frac{4d}{2\pi}\right)^2 \left[\frac{1}{V_1} + \frac{1}{V_2}\right] \tag{17}$$

The hydraulic natural frequency for the 70-m antenna is defined as

$$f_{\text{hydraulic}} = \frac{1}{2\pi}\sqrt{\frac{e_t e_v \beta}{J}\left(\frac{4d}{2\pi}\right)^2 \left[\frac{1}{V_1} + \frac{1}{V_2}\right]} \tag{18}$$

which will be used to calculate the antenna inertia. The bulk modulus, β; volumetric displacement, d; and hydraulic resonance, $f_{\text{hydraulic}}$, are determined from test data as described below. The volumes V_1 and V_2, the trapped hydraulic fluid between the servo valve and the hydraulic motor ports, are given in [3] as 0.02455 m^3 (1498.1 $in.^3$) and 0.02457 m^3 (1499.6 $in.^3$), respectively. Thus, the reflected inertia, J,

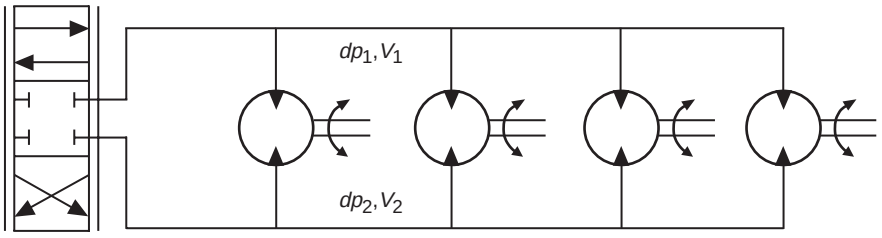

Fig. 2. Schematic of 70-m hydraulic lines leading to and from the hydraulic drive motors.

is the only unknown in the mathematical expression for the hydraulic natural frequency. Equation (18) may be rearranged to express the inertia, J, in terms of the other known variables:

$$J = \frac{e_t e_v \beta \left(\frac{4d}{2\pi}\right)^2 \left[\frac{1}{V_1} + \frac{1}{V_2}\right]}{(2\pi f_{\text{hydraulic}})^2} \tag{19}$$

or

$$J = \frac{K}{(2\pi f_{\text{hydraulic}})^2} \tag{20}$$

where K is from Eq. (17).

A. The Bulk Modulus

The bulk modulus, β, is related to the wave speed, c_0, and the density, ρ, of the hydraulic fluid (see [4]):

$$c_0 = \sqrt{\frac{\beta}{\rho}} \tag{21}$$

or,

$$\beta = c_0^2 \rho \tag{22}$$

The wave speed, c_0, may be expressed as the time, T, that a pressure wave travels the distance from the valve to the motor, L:

$$\beta = \left(\frac{L}{T}\right)^2 \rho \tag{23}$$

The time variable, T, or period, is equal to half of the time that it takes to complete one pressure oscillation cycle, T_p:

$$T = \frac{T_p}{2} \tag{24}$$

but,

$$T_p = \frac{1}{f_p} \tag{25}$$

Since the pressure or (slosh) frequency, f_p, is the reciprocal of the period, the expression may be restated as the following:

$$\beta = (2Lf_p)^2 \rho \tag{26}$$

The "slosh" frequency, f_p, may be described as the following: As the servo valve is suddenly opened, a pressure wave runs along the hydraulic line until it hits the hydraulic motor port where the pressure transducer resides. The wave then reflects backwards towards the valve to begin the cycle over again. In this discussion, the fluid's pressure cycle is termed the slosh frequency. Hydraulic lines are very lightly damped, so the signature frequencies of oscillation remain even after the servo valve is closed. Each hydraulic line length has its own signature frequency. An FFT of the hydraulic line pressure traces will separate the hydraulic line frequencies into their component parts. The longest hydraulic line will have the lowest slosh frequency, and the shortest hydraulic line will have the highest slosh frequency.

Figure 3 shows slosh frequencies of hydraulic lines measured after the servo valve was suddenly opened and then closed. An FFT of these waveforms is given in Fig. 4. The highest frequency is given as 46.3 Hz,

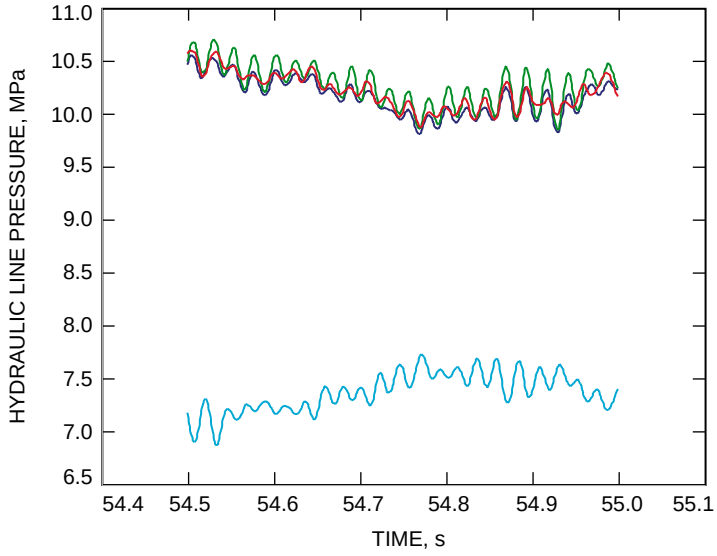

Fig. 3. A time plot of 70-m antenna hydraulic line pressures after the servo valve was suddenly closed.

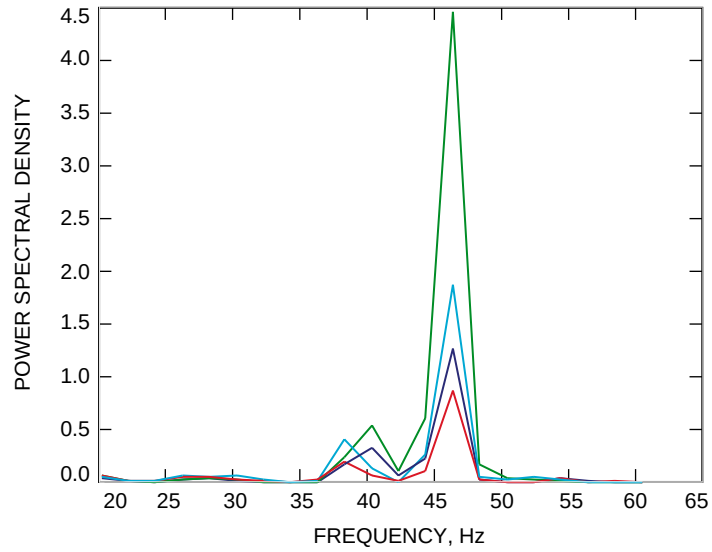

Fig. 4. A spectral plot of 70-m antenna hydraulic line pressures after the servo valve was suddenly closed. The lowest and highest slosh frequencies are 33.3 and 46.3 Hz, respectively.

and the lowest frequency is given as 38.3 Hz from the test data. The shortest hydraulic line length is 13.11 m (516 in.), and the longest line length is 15.60 m (614 in.). The hydraulic fluid density is given as 850 kg/m^3 (7.95×10^{-5} lbf-s^2/in.^{4}) (see [3]).

The insertion of the density, line length, and frequency values into Eq. (26) determines the bulk modulus: 1245.5 MPa (180,643 lbf/in.^{2}) for the shortest line and 1212.5 MPa (175,857 lbf/in.^{2}) for the longest hydraulic line.

B. Hydraulic Natural Frequency

The hydraulic resonance frequency, $f_{\text{hydraulic}}$, of 0.97 Hz was acquired from test data taken in October 1999. In this test, the 70-m antenna was instrumented with a pressure sensor at the inlet and outlet ports of each hydraulic motor. A triangle wave command was issued to the servo valve. The axis speed was measured by tachometers on each hydraulic drive. The difference between the inlet and outlet pressures is directly proportional to the driving torque of the hydraulic motor. The ringing or oscillations of hydraulic pressure traces are composed of hydraulic and structural resonance frequencies of the system. Figures 5 and 6 show the individual torques of each motor as well as the sum of all motor driving torques on the antenna axis. The antenna axis rate is measured by tachometer. The hydraulic and structural resonance frequencies can be seen in the torque summation traces that are depicted in Figs. 5 through 8. An FFT of the summation of torques decomposes it into a spectrum of frequencies. From this spectrum of frequencies, the hydraulic natural frequency may be extracted. It is difficult to separate the structural resonances from the hydraulic resonance. For this reason, the hydraulic natural frequencies from two antenna drive conditions—a high-speed ramp command and a low-speed ramp command—were evaluated in Figs. 9 and 10 for a spectral comparison; the eigenvalues from the JPL antenna structural model were used to eliminate certain frequencies near the expected range of resonance. The eigenvalues are the predicted structural resonant frequencies. No structural resonances are predicted to occur below 1.75 Hz on the azimuth axis of rotation.

C. Hydraulic Motor Displacement and Motor Efficiencies

The hydraulic motor parameters were determined by a test conducted at Fluid Technologies Inc. of Stillwater, Oklahoma, in November of 1999. Volumetric displacement, d, was measured to be 38.329 cc/rev

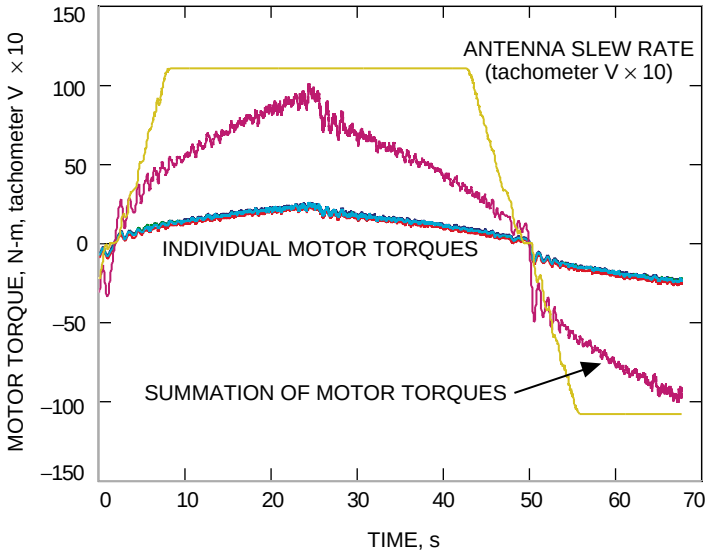

Fig. 5. A time plot of individual and total torque of the elevation-axis hydraulic motors and antenna slew rate during a high-speed ramp command.

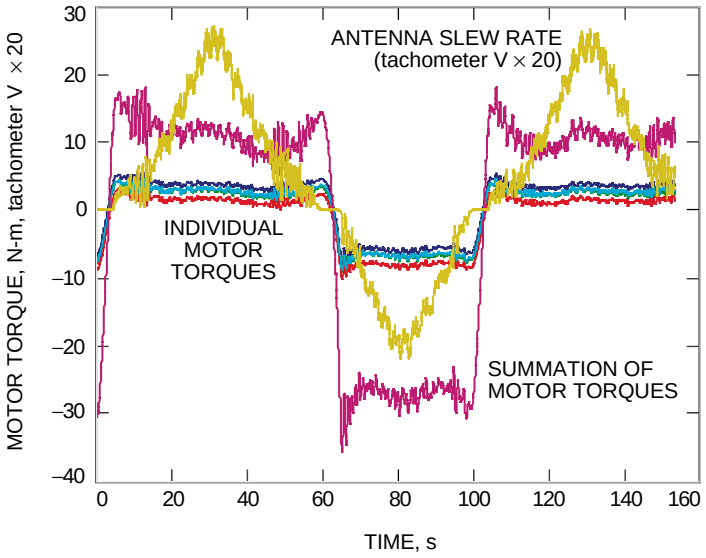

Fig. 6. A time plot of individual and total torque of the elevation-axis hydraulic motors and antenna slew rate during a low-speed ramp command.

(2.339 in.^{3}/rev); motor torque efficiency, e_t, was measured as 0.938; and motor volume efficiency, e_v, was measured as 0.9412.

D. Determination of 70-Meter Antenna Reflected Inertia and Inertia Ratio from Hydraulic Resonance Data

Combining the known variables into Eq. (19) and solving for the reflected antenna inertia, J, yields a value of 1.45 kg-m^2 (1.07 lbf-ft-s^2). The motor-to-load inertia ratio, R_{MtoL}, is as follows:

$$R_{\mathrm{MtoL}} = \frac{J_{\mathrm{motor}}}{J_{\mathrm{reflected}} - J_{\mathrm{motor}}} \tag{27}$$

Equation (27) yields a value of 4.63 for R_{MtoL}.

IV. 70-Meter Antenna Inertia Determination by Impulse and Momentum Considerations

The impulse/momentum equation will be derived from Newton's equation of motion for rotational bodies. This equation will be used to calculate the 70-m antenna's inertia using the previously discussed 70-m test data from October 1999. Other supplemental antenna data were taken in December 2000 to determine antenna frictions. Antenna friction is needed to determine how much drive torque actually goes to moving the antenna. Newton's equation for rotational motion, if integrated on both sides, is as follows:

$$\sum T = J\alpha \tag{28}$$

where $\sum T$ is the summation of torque or total torque applied to the 70-m reflected inertia, J, and α is a constant rate of angular acceleration:

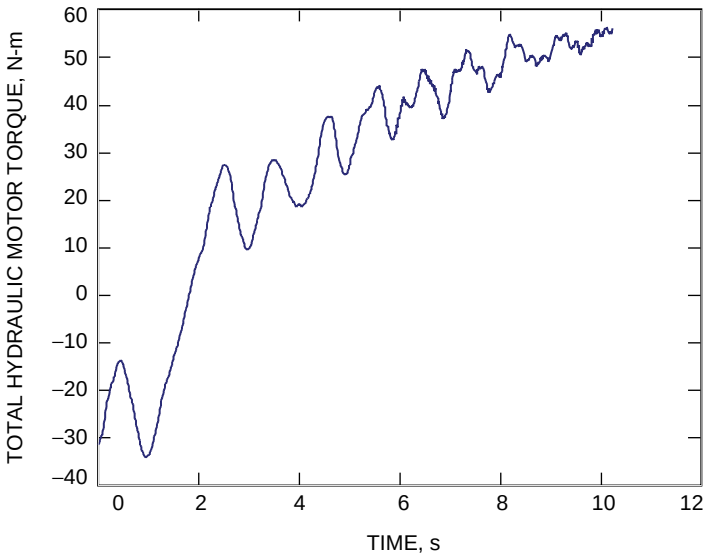

Fig. 7. A time plot of the total torque of the elevation-axis hydraulic motors during a high-speed ramp command.

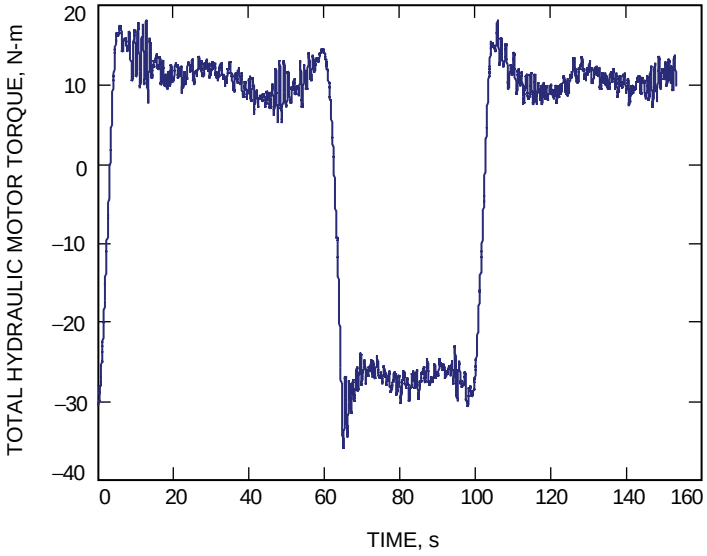

Fig. 8. A time plot of the total torque of the elevation-axis hydraulic motors during a low-speed ramp command.

$$\int \sum T dt = \int J\ddot{\theta} dt \tag{29}$$

$$\int \sum T dt = J\left[\dot{\theta}_2 - \dot{\theta}_1\right] \tag{30}$$

where $\dot{\theta}_1$ is the speed of the antenna at the beginning of the applied torque and $\dot{\theta}_2$ is the angular speed at the end of the applied torque. The integral of Newton's equation states that the impulse is equal to the change in the angular momentum. The impulse is defined as the integral of the driving torque of

the hydraulic motors over time. The momentum is the product of the antenna inertia and the angular rate of speed of the antenna. The change in the momentum is the reflected inertia times the difference of angular speed at the beginning of the applied torque subtracted from the angular speed at the end of the applied torque. The reflected antenna inertia, J, may be expressed from Eq. (30) as follows:

$$J = \frac{\int \sum T dt}{\left[\dot{\theta}_2 - \dot{\theta}_1\right]} \tag{31}$$

Antenna tachometer data, shown in Fig. 5, measure the speed of the antenna, although the tachometer is physically located on a different axis than the motor. The tachometer outputs 157 V per 600 rpm. The

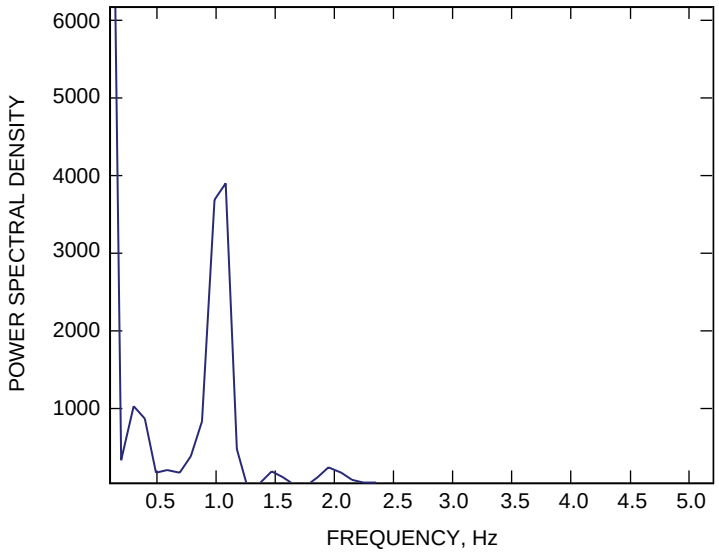

Fig. 9. A spectral plot of the total torque of the elevation-axis hydraulic motors during a high-speed ramp. The primary (hydraulic) frequency is approximately 1 Hz.

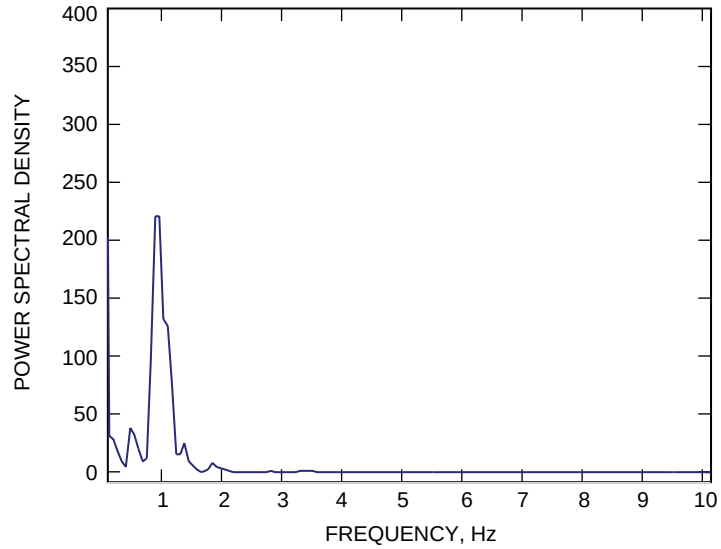

Fig. 10. A spectral plot of the total torque of the elevation-axis hydraulic motors during a low-speed ramp. The primary (hydraulic) frequency is approximately 1 Hz.

tachometer output plateaus in Fig. 5 because its output exceeds the data acquisition recorder input limit of approximately 10 V. The hydraulic motors turn at a rate of 130/23 times faster than the tachometers. The motor turns faster because of the gear ratio between the tachometer and the motor axes. Thus, the conversion factor for converting tachometer volts to motor radians per second is as follows:

$$\frac{600}{157}\left(\frac{\text{rev}}{V}\frac{1}{\text{min}}\right)\frac{1}{60}\left(\frac{\text{min}}{S}\right)\frac{2\pi}{1}\left(\frac{\text{rad}}{\text{rev}}\right)\frac{130}{23} = 2.261\left(\frac{\text{rad}}{S-V}\right) \tag{32}$$

Pressure transducers measure the driving torque of the hydraulic motor shown in Fig. 5 that is mathematically expressed as the left-hand side of Eq. (29). The motor's pressure is related to the motor's torque by Eq. (9). However, some of the driving torque is consumed by antenna friction. This means that the driving torque, applied by the hydraulic motors, does not totally translate into acceleration of the antenna. Frictional torques must be subtracted from the driving torques within the impulse integration.

On the elevation axis, the antenna dish is counterbalanced with a weight on the opposing side of its pivot point. The dish and counterweight do not exactly counterbalance each other. This condition creates an offset torque on the elevation axis. The result is that the offset torque either helps or hinders the motion of the antenna. In summary, the torque applied to the antenna is comprised of several components:

$$\sum T = T_{\text{drive}} + T_{\text{friction}} \pm T_{\text{offset}} \tag{33}$$

where T_{drive} is the driving torque, T_{friction} is the antenna frictional torques, and T_{offset} is the offset torque for the elevation axis. The antenna friction is comprised of three components: a steady-state component known as coulomb friction, static or breakaway friction, and viscous friction. Viscous friction is dependent upon the rotational speed of the antenna.

A. Offset Torque Elimination

The offset torque must be eliminated from elevation-axis data before the reflected inertia can be determined. If one assumes that the offset torque is biased to the counterweight side of the pivot point rather than the dish side of the pivot point, when the antenna dish is moved upward the offset torque assists the driving torque. If the antenna dish is moved downward, the offset force opposes the driving force. In order to eliminate the offset torque from calculations, the antenna torque for upward motion and antenna torque for downward motion, over the same angular path, must be added together and then the result divided by two. The contribution of the offset torque for each direction cancels with the other when this operation is performed. Two integrations are performed on the total motor torque curve to find the antenna's inertia. Then the results are added together and scaled by a factor of one-half. The first integral lower limit occurs where the antenna's rate initially becomes positive in Fig. 5. The first integral upper limit is where the tachometer data plateau slightly above 10 V. The second integral lower limit is where the tachometer data begin to transition downwardly from the 10-V plateau in Fig. 5. The second integral upper limit is where the number of time divisions matches the time divisions in the first integration.

B. Antenna Testing for Frictional Torque

Antenna friction values may be obtained by performing constant speed tests or slow ramp tests with the antenna's rate loop in operation.

1. Constant Speed Tests. The justification for the constant speed test is found in Newton's equation for rotational motion: The summation of the external torques is equal to the rotational inertia times the angular rate of acceleration. However, for constant speed conditions, the angular acceleration is

equal to zero. So, the summation of all the external forces equals zero. Thus, Eq. (33) can be rearranged to state that the driving torque equals the frictional torque plus or minus the offset torque:

$$T_{\text{drive}} = T_{\text{friction}} \pm T_{\text{offset}} \tag{34}$$

During 70-m antenna constant speed testing, a bipolar symmetrical square wave was applied to the servo rate loop before the summing junction. This allowed the rate loop to regulate to the commanded speeds. The symmetrical bipolar square wave causes the antenna to rotate at a constant speed in one direction and then causes it to reverse that direction while running at the same speed. Several cycles were conducted to ensure that repeatable results occurred. This cycle results in one data point for the antenna friction at the commanded speed. Because the antenna viscous friction is speed dependent, multiple cycles at different square-wave amplitudes must be conducted to ascertain the antenna frictions at other speeds. When the testing is completed, an antenna friction-versus-angular speed curve may be plotted. The curve's intercept on the y-axis shows the coulomb friction torque (i.e., the steady-state friction at zero speed). The curve's slope defines the coefficient for the viscous friction term (assuming a linear curve). Only two data points were available from 70-m antenna constant speed tests. These two points yield a slope of 5.21 N-m/rpm (46.1 in.-lbf/rpm) and coulomb friction value, or y-intercept, of 69.49 N-m (615.00 in.-lbf).

2. Slow Ramp Tests. The slow ramp test is a second approach for determining antenna friction. A bipolar symmetrical triangle wave is applied to the servo system rate loop before the summing junction. A signal input before the summing junction allows the antenna to follow the servo valve commands. The physical basis for a slow ramp is that the driving torque of the antenna is gradually increased until the antenna begins to move. The value of the torque at the instance when motion begins is called the breakaway friction. Breakaway friction is normally higher than the friction after the motion begins. After breakaway, the driving torque is commanded to continue to ramp up the antenna speed at the same rate. The torque that remains after antenna motion begins is called coulomb friction. Figure 6 shows the results of slow ramp testing. Hydraulic motor torque is measured by pressure transducers in each motor port. The hydraulic motor port pressure is related to its output torque by Eq. (9). The torque summation curve shows the total torque applied to the elevation axis. The antenna motion is measured by tachometers. The tachometer trace follows the commanded bipolar triangle waveform pattern that was input to the servo valve. Like the constant speed test results, the torque values must be processed to eliminate the offset torque. The measured coulomb torque value of 14.12 N-m (125 in.-lbf) during upward motion of the antenna must be added to the measured coulomb torque value of 25.42 N-m (225 in.-lbf) during the downward motion of the antenna. The result was divided by two, giving a coulomb friction value of 19.77 N-m (175 in.-1bf).

3. Coulomb Friction Discrepancy. It is not known why the value for coulomb friction in the constant speed tests differs from the friction results from the slow ramp test. Perhaps the relationship between the antenna friction and the antenna speed is not linear, as originally assumed. Further tests of the antenna are necessary to better define the antenna friction-versus-antenna speed curve. The 70-m antenna inertia is calculated in the following using both values for coulomb friction.

C. Impulse/Momentum Antenna Inertia Ratio Calculation

The inertia calculation using Eq. (30) with the drive torque data (hydraulic motor port pressure measurements from Fig. 5), drive friction data (constant speed test results), and antenna tachometer data from Fig. 5 yielded a moment of inertia of 1.668 kg-m^2 (1.23 lbf-ft-s^2). The same inertia calculation, using the friction results from the slow ramp tests from Fig. 6 instead of the friction results from constant speed tests, yields a reflected inertia of 1.45 kg-m^2 (1.07 lbf-ft-s^2). The motor-to-load ratio as computed from Eq. (27) is 2.51 for the constant speed inertia data, while it is 4.63 for the slow ramp inertia data.

V. Summary

The 70-m reflected inertia was calculated using three methods in an effort to perform inertia matching for an upgraded servo system. The first method computed the antenna inertia using antenna mass properties, component volumes from drawings, and densities. The second method computed the inertia from a mathematical expression for the hydraulic resonance. The third method computed the antenna inertia from impulse and momentum considerations. The first method yielded a value of 1.776 kg-m^2 (1.3 ft-lbf-s^2); the second method yielded a value of 1.45 kg-m^2 (1.07 ft-lbf-s^2); and, finally, the third method yielded values of 1.668 kg-m^2 (1.23 lbf-ft-s^2) and 1.45 kg-m^2 (1.07 lbf-ft-s^2). The servo motor-to-load inertia ratio results ranged from 2.09 to 4.6. Of the three methods of determining antenna inertia, the hydraulic resonance and the impulse/momentum methods are the most credible because they are based upon actual test data with fewer assumptions and approximations. Each method indicates that the 70-m antenna's motor-to-load inertia is greater than the one-to-one ratio that is considered by industrial servo control experts to be ideal for an optimal tracking response.

Acknowledgments

The author would like to thank Abner Bernardo, Hal Ahlstrom, Peter Hames, David Schaller, and Bob Wallace for planning, conducting, and recording 70-m servo system tests. Thanks to Najib Kasti for calculating the structural resonance frequencies of the 70-m antenna. A special thanks to Wodek Gawronski for reviewing and editing this article and for sharing his extensive knowledge of MATLAB analysis tools.

References

[1] J. J. D'Azzo and C. H. Houpis, *Feedback Control System Analysis and Synthesis*, Second Edition, New York: McGraw Hill Book Company, pp. 28–31, 1966.

[2] E. A. Avallone and T. B. Baumeister III, *Marks' Standard Handbook for Mechanical Engineers*, Ninth Edition, New York: McGraw Hill, Inc., pp. 6–7, 1987.

[3] R. D. Bartos, "Dynamic Modeling of Fluid Transmission Lines of the DSN 70-Meter Antennas by Using a Lumped Parameter Model," *The Telecommunications and Data Acquisition Progress Report 42-109, January–March 1992*, Jet Propulsion Laboratory, Pasadena, California, pp. 163–168, May 15, 1992. http://tmo.jpl.nasa.gov/tmo/progress_report/42-109/109N.PDF

[4] W. Russell and P. E. Henke, *Fluid Power Systems and Circuits*, fourth edition, edited by Tobi Goldoftas, Cleveland, Ohio: Penton Publishing Inc., pp. 352–353, September 1983.